Chapter 5

Cloud Microphysics

5.1 Nucleation of hydrometeors

5.1.1 Heterogeneous nucleation of cloud droplets

When a parcel of moist air rises to the condensation level, the liquid phase initially takes the form of small droplets which form, or *nucleate* on water-soluble aerosol particles. The number of droplets which form is therefore a strong function of the concentration, constitution, and size distribution of such aerosols. As the relative humidity increases, these particles grow by absorption of water molecules, forming a concentrated solution. However, further growth into cloud droplets depends on criteria which we now discuss.

Growth of these aerosols and droplets occurs when the actual vapor pressure of water exceeds the saturation vapor pressure relative to the droplet in question. This droplet-specific saturation vapor pressure differs from the standard saturation vapor pressure as the result of two competing processes: (1) The Kelvin effect causes the saturation vapor pressure over the curved surface of the droplet to be greater than that over a flat water surface. (2) Raoult's law tells us that the vapor pressure over water containing a solute is less than that over pure water.

Kelvin effect

In the chapter on thermodynamics we learned, contrary to the common assertion, that the saturation vapor pressure of water vapor is actually a (weak) function of the environmental pressure p. We can write this dependence in

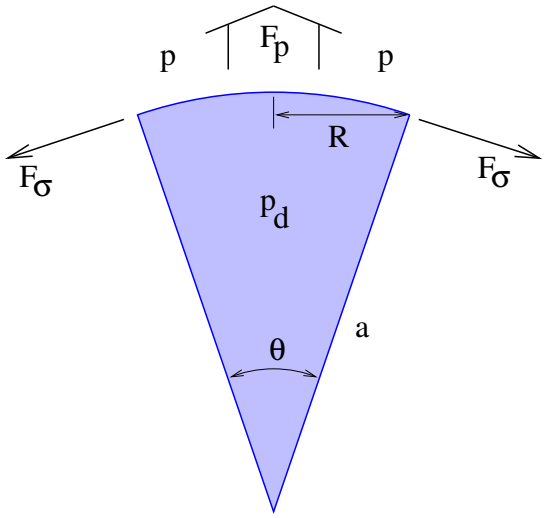

Figure 5.1: The pressure p_d inside a cloud droplet of radius a is greater than the surrounding pressure p due to the surface tension. the force of surface tension F_σ on a circular region of droplet surface of radius R is balanced by the pressure force across the surface.

the form

$$e_S(T, p) = e_S(T) \exp[p/(R_V T \rho_w)], \tag{5.1}$$

where $e_S(T)$ is the saturation vapor pressure at zero pressure and temperature T (and is the commonly quoted expression for saturation vapor pressure; see the chapter on thermodynamics). This pressure dependence becomes important in small droplets in which the pressure inside the drop is enhanced over the pressure in the surrounding air. This pressure difference is called the Kelvin effect.

Figure 5.1 shows how this increased pressure inside the drop is produced. Due to surface tension, a force per unit length σ is exerted across the boundary of the circular region of drop surface illustrated in cross-section in this figure. The total downward component of this force is $2\pi R\sigma \sin(\theta/2)$, which in the small angle approximation becomes $\pi R\sigma\theta = 2\pi R^2\sigma/a$, since $\theta \approx 2R/a$. The upward pressure force on the surface is $\approx \pi R^2(p_d - p)$ where p_d is the pressure inside the drop and p is the pressure of the surrounding air. Equating these two forces tells us that

$$p_d - p = 2\sigma/a. \tag{5.2}$$

Since $\sigma = 7.5 \times 10^{-2}$ N m^{-1} for water near the freezing point, $p_d - p = 1500$ hPa for a droplet of radius $a = 10^{-6}$ m, a not inconsiderable pressure difference.

In equation (5.1), the pressure is actually the pressure p_d in the liquid inside the drop. The saturation vapor pressure over a droplet of radius a is therefore

$$e_S(T, p_d) = e_S(T, p) \exp[2\sigma/(R_V T \rho_w a)] \approx e_S(T)(1 + a_k/a), \tag{5.3}$$

where the approximation of the exponential function by a first order Taylor series is quite accurate for the range of values encountered in the atmosphere and where $a_k = 2\sigma/(R_V T \rho_w)$ ($\approx 1.2 \times 10^{-9}$ m at $T = 273$ K). We have also approximated $e_S(T, p)$ by $e_S(T, 0) = e_S(T)$.

Reduction of saturation vapor pressure by solute

Raoult's law indicates that the saturation vapor pressure of water containing a solute is reduced from the pure water value by the *activity*

$$X = \frac{n_w}{n_w + n_s}, \tag{5.4}$$

where n_w is the number of moles of water in the droplet and n_s is the number of moles of solute. Raoult's law isn't particularly accurate for electrolytes, such as the typical salts encountered in atmospheric aerosols, but we will use it here for the purposes of illustration. A more exact treatment may be found in Pruppacher and Klett (1978). We further assume that $n_s \ll n_w$, so that we can approximate the activity as

$$X = 1 - n_s/n_w. \tag{5.5}$$

We now set $n_s = M_s/m_s$ where M_s is the mass of solute in the droplet and m_s is its molecular weight. A similar expression for the number of moles of water in the droplet yields $n_w = M_w/m_V = 4\pi a^3 \rho_w/(3m_V)$, where m_V is the molecular weight of water substance and where we assume that the density of the solute is unchanged from the density ρ_w of pure water. The activity thus becomes

$$X = 1 - \frac{3 m_V M_s}{4\pi m_s \rho_w a^3} \equiv 1 - \frac{a_s^3}{a^3} \tag{5.6}$$

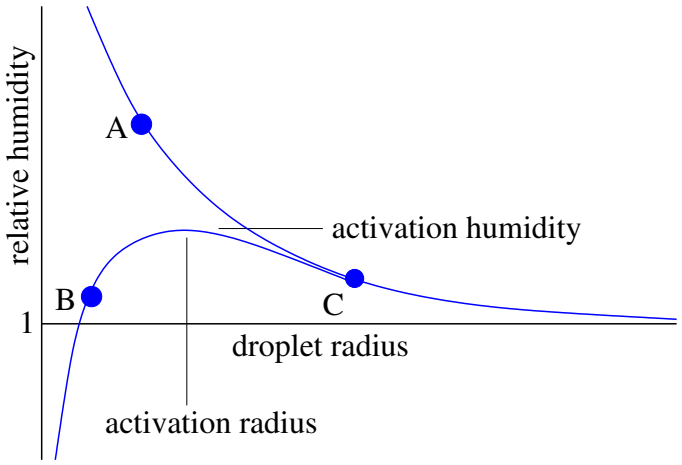

Figure 5.2: Schematic plots of equilibrium relative humidity versus droplet radius for pure water (curve AC) and solution (curve BC). The activation relative humidity is generally less than 1.01 and activation occurs typically for droplet radii less than 1 μm.

where $a_s = [3m_V M_s/(4\pi m_s \rho_w)]^{1/3}$, and the saturation vapor pressure over a droplet consisting of a solution with activity X is

$$e_S(T, p_d, X) = X e_S(T, p_d). \tag{5.7}$$

Köhler curves

Combining the Kelvin effect and Raoult's law results in the expression

$$\mathcal{H}_e = e_S(T, p_d, X)/e_S(T) \approx \left(1 + \frac{a_k}{a} - \frac{a_s^3}{a^3}\right), \tag{5.8}$$

where $\mathcal{H}_e$ is the *equilibrium relative humidity* for the droplet, or the value of the relative humidity relative to a flat surface of pure water which results in a vapor pressure equal to the saturated vapor pressure over the droplet of solution.

Figure 5.2 shows schematic plots of the equilibrium relative humidity as a function of droplet radius for droplets consisting of pure water (curve AC) and solute (curve BC). If the actual humidity is higher than the equilibrium humidity for the droplet's radius and solute concentration, then the

droplet will experience condensation and will grow. Conversely, if the actual humidity is less than this value, the droplet will evaporate.

The points A and C in figure 5.2 thus represent unstable equilibria, in that if the droplet radius should become slightly larger than the indicated value, the equilibrium relative humidity becomes less than the actual value, and the droplet grows further, thus departing more from the equilibrium point. Likewise, a radius slightly less than the equilibrium value produces accelerating evaporation. In contrast, the point B represents a stable equilibrium, with departures from the specified droplet radius resulting in a tendency to return to this radius.

If the relative humidity is increased to the *activation humidity* for a solute drop, as illustrated in figure 5.2, the drop radius will increase beyond the *activation radius* and the droplet will then undergo unbounded condensational growth. We say that the original aerosol is a *cloud condensation nucleus* or CCN and has become *activated*. This is the process of *heterogeneous nucleation*.

Homogeneous nucleation is the process by which a number of water molecules spontaneously aggregate by accident, thus forming a very small droplet. Very high values of the relative humidity are required for such droplets to grow, because their initial radius is so small and because they have no solute content to reduce their equilibrium relative humidity to a more reasonable value. Homogeneous nucleation rarely occurs in the atmosphere, as water-soluble aerosols are almost always available in sufficient quantities to produce enough heterogeneous nucleation to take up the available water vapor at vapor pressures only slightly above the saturation vapor pressure. It is for this reason that cloud models generally assume all water vapor in excess of that required to produce saturation over a pure, flat water surface to be instantly condensed.

Cumulus cloud updrafts in very clean air over oceans often nucleate 200 or fewer CCN per cubic centimeter, while comparable updrafts in contaminated air over land can produce one to two orders of magnitude higher droplet concentrations. This difference has significant consequences for the ability of cumulus clouds to produce precipitation in the two situations, as we shall see.

5.1.2 Ice nucleation

Cloud droplets do not freeze spontaneously when they are lifted above the freezing level by updrafts. In fact, spontaneous freezing does not occur until droplets are cooled to at least $-40°$ C. Most freezing in clouds therefore occurs by the action of *ice nuclei*.

Ice nuclei are aerosols which create ice crystals at temperatures below freezing by one of three mechanisms (Pruppacher and Klett, 1978): direct deposition onto the aerosol; freezing via an aerosol which has previously been incorporated into the droplet; and freezing which occurs when an aerosol in the surrounding air comes in contact with the droplet. The effectiveness of ice nuclei becomes greater as the temperature decreases. According to Young (1993), complete freezing initiated by commonly present ice nuclei generally occurs in the atmosphere by $-20°$ C. Particularly effective ice nuclei such as silver iodide crystals can initiate freezing at temperatures as warm as $-4°$ C.

Many facets of ice nucleation are still not well understood; it is a field filled with formidable observational, experimental, and theoretical difficulties.

5.2 Diffusive growth

Here we consider the growth of water droplets, and briefly, the growth of ice crystals by diffusive processes.

5.2.1 Growth of water droplets

We now investigate the diffusional growth of small water drops in the presence of supersaturation, i. e., a relative humidity $\mathcal{H}$ greater than the equilibrium relative humidity $\mathcal{H}_e$ of the droplet in question. As illustrated in figure 5.3, latent heat released at the surface of the drop by condensation of the vapor must be exported diffusively.

Given a gradient in the density of water vapor ρ_V, the flux of water vapor is

$$\mathbf{F}_V = -D\nabla\rho_V, \tag{5.9}$$

where D is the diffusivity of water molecules in air. Adjustment of the water vapor distribution can be shown in this case to occur very rapidly compared to other possible processes, which means that to a good approximation the

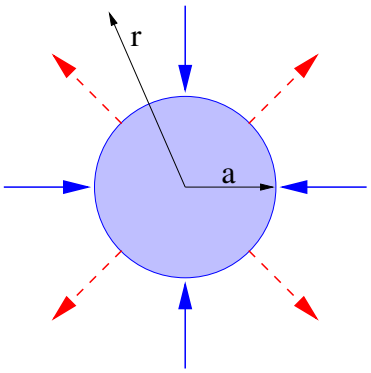

Figure 5.3: A droplet growing by diffusion imports water vapor (inward arrows) and exports the latent heat produced by condensation of the vapor on the drop surface (outward arrows).

water vapor distribution satisfies the time-independent diffusion equation $\nabla^2 \rho_V = 0$. This has the spherically symmetric solution

$$\rho_{Vr} = \rho_V + \frac{(\rho_{Va} - \rho_V)a}{r}, \tag{5.10}$$

where ρ_{Vr} is the vapor density at radius r, with ρ_{Va} being the value at the surface of the droplet, and where ρ_V is now taken as the density far from the droplet. With this solution the radial component of the flux at the surface of the drop is

$$F_{Va} = \frac{D(\rho_{Va} - \rho_V)}{a}. \tag{5.11}$$

The time rate of change of the droplet mass M_d can be related to this flux:

$$\frac{dM_d}{dt} = -4\pi a^2 F_{Va}. \tag{5.12}$$

Given that for a spherical drop, $M_d = 4\pi a^3 \rho_w/3$ where ρ_w is the density of liquid water, this equation can be recast in terms of the time rate of change of the droplet radius. substituting equation (5.11), we find

$$a\frac{da}{dt} = -\frac{D(\rho_{Va} - \rho_V)}{\rho_w}. \tag{5.13}$$

The diffusive heat flux is

$$\mathbf{F}_H = -K\nabla T \tag{5.14}$$

and by the same arguments as made above, the temperature at radius r is

$$T_r = T + \frac{(T_a - T)a}{r} \tag{5.15}$$

where T_a is the temperature at the surface of the droplet and T is the temperature far from the droplet. The heat flux at the droplet surface is therefore

$$F_{Ha} = \frac{K(T_a - T)}{a}. \tag{5.16}$$

The sensible heat flow away from the droplet must just balance the latent heat flow toward the droplet, which means that the fluxes of vapor and heat are related by $F_{Ha} = -LF_{Va}$, where L is the latent heat of condensation. Thus, we have

$$K(T_a - T) = -LD(\rho_{Va} - \rho_V). \tag{5.17}$$

As long as the droplet radius is much greater than the mean free path of air molecules, i. e., greater than a micrometer or so, the air at the droplet surface will be saturated. By the ideal gas law,

$$\rho_{Va} = \frac{e_{Sd}(T_a)}{R_V T_a} \approx \frac{e_{Sd}(T_a)}{R_V T} \approx \frac{e_{Sd}(T)}{R_V T}\left[1 + \frac{1}{e_S}\frac{de_S}{dT}(T_a - T)\right], \tag{5.18}$$

where $e_{Sd}(T_a)$ is the saturation vapor pressure specific to the drop, at the droplet temperature. Several approximations have been made: the droplet temperature has been replaced by the temperature distant from the drop in the denominator, but not in the expression for the saturation vapor pressure, since the vapor pressure is a very sensitive function of the temperature; a Taylor series expansion has been used to write the saturation vapor pressure at temperature T_a in terms of the saturation vapor pressure at temperature T; finally, the droplet-specific saturation vapor pressure has been replaced by the vapor pressure over a flat, pure water surface in the first order term of the Taylor series.

Computing the logrithmic derivative of the saturation vapor pressure yields

$$\frac{1}{e_S}\frac{de_S}{dT} = \frac{L_L}{R_V T^2} \tag{5.19}$$

where L_L is the latent heat of condensation. Substituting this into equation (5.18) finally yields

$$\rho_{Va} = \frac{e_S(T)\mathcal{H}_e}{R_V T}\left[1 + \frac{L_L(T_a - T)}{R_V T^2}\right], \tag{5.20}$$

where we have set $e_{Sd}(T) = e_S(T)\mathcal{H}_e$. Recall that $\mathcal{H}_e$ is the equilibrium relative humidity over the drop (at temperature T) and $e_S(T)$ is the saturation mixing ratio over a pure, flat water surface at this temperature.

Substitution of equation (5.20) into equation (5.17) results in

$$T_a - T = -\frac{L_L D e_S(\mathcal{H}_e - \mathcal{H})}{K R_V T + L_L^2 D e_S/(R_V T^2)}, \tag{5.21}$$

where the minor additional approximation that $\mathcal{H}_e$ is set to unity where it occurs by itself. Between this equation and equations (5.13) and (5.17), we finally arrive at an expression for droplet growth:

$$a\frac{da}{dt} = \frac{r_S D(\rho/\rho_w)(\mathcal{H} - \mathcal{H}_e)}{1 + r_S(D/\kappa)[L_L^2/(C_{PD} R_V T^2)]} \equiv A. \tag{5.22}$$

In this equation we have defined the heat diffusion coefficent for air $\kappa = K/(\rho C_{PD})$ where ρ is the air density, and we have eliminated the saturation vapor pressure in favor of the saturation mixing ratio $r_S = e_S/(R_V T \rho)$. We refer to $\mathcal{H} - \mathcal{H}_e$ as the *supersaturation*.

The diffusivity of water vapor is a function of temperature and pressure,

$$D = 2.14 \times 10^{-5}(T/T_F)^{1.94}(p_R/p) \text{ m}^2 \text{ s}^{-1} \tag{5.23}$$

according to Pruppacher and Klett (1978), where $T_F = 273.15$ K and $p_R = 1000$ hPa. The diffusivity of heat and water vapor should scale the same way with respect to temperature and pressure. The ratio of the two is approximately

$$D/\kappa = 1.15. \tag{5.24}$$

Assuming that the right side of equation (5.22) takes on a constant value $A > 0$, the droplet radius will increase with time according to

$$a(t) = (2At)^{1/2} \tag{5.25}$$

and the droplet mass will obey

$$M_d(t) = \frac{4\pi a^3 \rho_w}{3} = \frac{4\pi(2At)^{3/2}\rho_w}{3}. \tag{5.26}$$

Thus, the rate of increase of droplet mass itself increases with time under these conditions. The implication of this result is that if condensation supplies mass to a fixed number of droplets at a constant rate, then the value of

the supersaturation $\mathcal{H} - \mathcal{H}_e$ must decrease with time. Thus, under normal circumstances, a parcel of air reaches a relatively high value of supersaturation just as condensation begins, and this supersaturation decreases as the resulting droplets grow in size.

The square-root dependence of droplet radius on time means that an initial size distribution of droplets will become narrower as droplets grow by diffusion. This has important consequences for the production of precipitation by collision-coalescence processes, as we shall see.

5.2.2 Bergeron process

As we noted earlier, liquid water droplets in clouds do not spontaneously freeze when they are lifted above the freezing level by updrafts. The freezing process is a gradual one, as some of the droplets encounter ice nuclei and freeze into ice crystals as a result. The Swedish meteorologist Tor Bergeron first realized that a mixed environment of supercooled droplets and a few ice crystals promotes rapid diffusional growth of the ice crystals as a consequence of the saturation vapor pressure over ice being lower than that over liquid water.

5.3 Accretional growth

Droplets and ice crystals produced by diffusional growth in the time available in a convective cloud are generally too small to fall out of the cloud and reach the ground. Precipitation is produced when small hydrometeors generated by the diffusion mechanism collide and stick together, resulting in composite particles with a greater fall velocity relative to the air parcel in which they are embedded and a greater resistance to evaporation as they fall through the unsaturated environment.

In order for collisions, and thus coalescence to occur, the distribution of fall velocities of hydrometeors must be broad enough for there to be significant differential motion between them. Only if this is true can hydrometeors collide with each other. Thus, the first topic we take up is how to estimate hydrometeor fall velocities.

5.3.1 Hydrometeor fall velocities

Pruppacher and Klett (1978) and other references on cloud physics provide detailed information on *terminal fall speed* w_T, i. e., the equilibrium fall speeds of hydrometeors relative to the air parcel in which they are imbedded of all sorts of hydrometeors. Here we confine ourselves to understanding the basic principles that determine these fall speeds.

In the equilibrium case, we have a balance between the force of gravity on the hydrometeor and the drag force of the air. As a hydrometeor gets bigger, it takes longer to establish this equilibrium, but in most cases the transient regime is unimportant. Thus, we confine ourselves to the equilibrium situation.

An important parameter in determining the character of the flow past a hydrometeor is the *Reynolds number* of the flow. The Reynolds number is an estimate of the ratio of inertial to viscous forces in a flow:

$$\mathrm{Re} \approx \frac{|\mathbf{v} \cdot \nabla \mathbf{v}|}{|\nu \nabla^2 \mathbf{v}|}. \tag{5.27}$$

In estimating this dimensionless number, we approximate spatial derivatives by inverse lengths and velocities by typical velocity values occurring in the problem. Here we assume that $\nabla \to 1/a$ where a is the hydrometeor radius (or other characteristic dimension for a non-spherical hydrometeor) and $|\mathbf{v}| \to w_T$, resulting in

$$\mathrm{Re} = \frac{w_T a}{\nu}. \tag{5.28}$$

Low Reynolds number

Small particles fall slowly and therefore exhibit low Reynolds number flow around them. In this case the drag force is dominated by the viscous term relative to the pressure term, which tends to scale with the inertial term $\mathbf{v} \cdot \nabla \mathbf{v}$. An exact solution to the viscous drag may be obtained in this case, but an approximate form for the drag which scales with the actual drag may be obtained using simple arguments.

The viscous stress on the surface of the drop is equal to the strain rate at the surface of the drop, dotted with the outward normal to the droplet surface, times the dynamic viscosity μ. The strain is produced by the droplet itself, and a scale analysis indicates that it scales with w_T/a, where a is the drop radius. Multiplying this by the viscosity and a^2, which is proportional

to the surface area of the drop leads to an estimate for the viscous drag: $F_d \approx \mu a w_T$. The actual drag obtained from a detailed calculation is

$$F_d = 6\pi\mu a w_T. \tag{5.29}$$

Equating this to the force of gravity on the drop $F_g = M_d g = 4\pi a^3 \rho_w g/3$ yields

$$w_T = \frac{2\rho_w g a^2}{9\mu}, \tag{5.30}$$

where g is the acceleration of gravity and ρ_w is the density of liquid water.

The Reynolds number may be evaluated retrospectively in order to determine the range of validity of this equation,

$$\mathrm{Re} = \frac{2\rho_w g a^3}{9\rho\nu^2}, \tag{5.31}$$

where we have written the dynamic viscosity in terms of the kinematic viscosity ν: $\mu = \rho\nu$. The Reynolds number appears to increase with decreasing density, but this fails to take into account that the kinematic viscosity itself is inversely proportional to the density, which means that the Reynolds number actually decreases with decreasing density! Using typical sea level values $\rho = 1.2$ kg m^{-3} and $\nu = 1.5 \times 10^{-5}$ m^2 s^{-1}, we find that

$$a(\mathrm{Re}) = 5.0 \times 10^{-5} \mathrm{Re}^{1/3} \text{ m}. \tag{5.32}$$

Thus drops up to about 25 μm in radius have Reynolds numbers of 0.1 or less, and droplets with this radius have a terminal velocity of about 0.075 m s^{-1}. Below this radius terminal velocity scales as the square of the droplet radius.

High Reynolds number

At high Reynolds number the pressure part of the stress exceeds the viscous part. In this case the difference between the pressure on the front and rear of the drop is the primary source of drag. The pressure at the very front of the drop will be $\rho w_T^2/2$ greater than the ambient pressure, a result which may be obtained using the Bernoulli equation and assuming that the flow velocity there is zero. The pressure on the rear of the drop varies with Reynolds number, but is generally not too far from the ambient pressure at high Reynolds number.

Dropping numerical factors, we can therefore estimate the drag force on the drop to be of order $F_d \approx a^2 \rho w_T^2$, since the projected area of the drop scales with a^2. We write this

$$F_d = C_D \rho a^2 w_T^2 \tag{5.33}$$

where the *drag coefficient* C_D is a dimensionless parameter of order unity which is a function only of Reynolds number. Equating this to the force of gravity on the drop yields a terminal velocity equal to

$$w_T = \left(\frac{4\pi \rho_w g a}{3 \rho C_D} \right)^{1/2}. \tag{5.34}$$

The Reynolds number therefore becomes

$$\mathrm{Re} = \left(\frac{4\pi \rho_w g a^3}{3 \rho \nu^2 C_D} \right)^{1/2}, \tag{5.35}$$

where this is an implicit equation, as C_D is itself a function of Reynolds number. Solving for droplet radius, we find

$$a(\mathrm{Re}) = 1.9 \times 10^{-5} C_D^{1/3} \mathrm{Re}^{2/3} \text{ m}. \tag{5.36}$$

If $C_D = 1$ and $\mathrm{Re} = 300$, then $a \approx 0.85$ mm and $w_T \approx 5.4$ m s^{-1}, which is not too far away from the measured sea level value (see, e. g., Gunn and Kinzer, 1949). Between Reynolds numbers of 0.1 and 300, there is no simple solution, but measurements have been fit to convenient equations by Beard (1976).

Distortion of large drops

When differences in pressure on different parts of a rain drop become comparable to the pressure excess inside a drop due to surface tension, then the drop deforms. Equating the surface tension-induced pressure excess inside a drop from equation (5.2) to the pressure excess at the nose of a drop, $\rho w_T^2/2$, and then eliminating w_T with equation (5.34) results in a critical radius

$$a_c = \left(\frac{3 C_D \sigma}{\pi \rho_w g} \right)^{1/2} \approx 1.3 \text{ mm}, \tag{5.37}$$

where as usual we have assumed sea level values and $C_D = 1$. Droplets with radii of this order or larger are subject to significant distortion by pressure forces.

Since the highest pressure exists on the bottom of the falling drop and the lowest pressure exists around the horizontal periphery, large rain drops tend to be distorted into the shape of a horizontally oriented pancake. Drops greater than about 4 mm in radius cannot exist due to these pressures, and even smaller drops are sometimes disrupted, as we shall see below. The greater cross section presented by distorted rain drops causes additional drag over that which would have occurred if the drop were spherical. This effect increases with droplet mass, resulting in a maximum terminal velocity of rain drops at sea level of order 10 m s^{-1}.

Ice hydrometeors

Ice hydrometeors are not subject to disruption by pressure forces as are liquid drops, so in principle (and occasionally in practice) they can become bigger than rain drops. However, ice hydrometeors are often less dense than liquid water, and this needs to be taken into account in the calculation of terminal velocities as well. In addition, smaller ice crystals can differ significantly from the spherical shape we have assumed so far, which makes calculation of their terminal velocities difficult. However, the strongest deviations from a spherical shape occur for small crystals resulting from diffusional growth, where the terminal velocities tend to be small in any case.

5.3.2 Precipitation production

Precipitation is produced when small hydrometeors produced by diffusive growth collide and stick together. We first list the types of precipitation particles produced and the mechanisms by which this production occurs. We then investigate time scales for the precipitation production by collision and subsequent coalescence.

Types of precipitation particles

- *Warm rain* arises from collisions between droplets. Calculations of this process are often unable to explain the rapidity with which it happens

under certain circumstances, such as moist tropical conditions. A hypothesis which has gone in and out of favor over the years is that warm rain is initiated by ultra-giant salt nuclei, which are capable of growing much larger than the usual droplets via diffusional growth. Such nuclei might be produced by evaporation of spray from breaking ocean waves.

- *Snowflakes* result from the aggregation of ice crystals created by the Bergeron process. The existence of aggregates of pristine crystals indicates that precipitation formation took place in the absence of supercooled liquid water once the ice crystals have exhausted the initial supply via diffusive transfer. Snowflakes have a very low density, and hence fall relatively slowly through the air (≈ 1 m s^{-1}).

- *Graupel* consists of ice crystals or snowflakes which have encountered additional supercooled liquid. When such droplets impact these particles, they freeze instantly, a process called *riming*. Riming tends to fill in the gaps between crystals, resulting roughly spherical particles with densities higher than that of snowflakes, but less than that of pure ice. When graupel encounters supercooled droplets with radii of at least 12 μm between temperatures of -3 C and -8 C, the freezing process can cause the ejection of numerous small ice crystals. This is called the Hallett-Mossop ice multiplication process (Hallett and Mossop, 1974). The Hallett-Mossop process can generate far more ice crystals than can be produced by the typical environmental concentration of ice nuclei. These ice crystals can then grow via the Bergeron process and serve as nuclei for additional graupel particles, etc.

- *Hail* is produced when graupel encounters especially high concentrations of supercooled water. The latent heat release exceeds the ability of the hailstone to transfer heat to the environment, raising the temperature of the hailstone to the freezing point. Freezing is thus delayed, which means that the liquid water can easily flow into the remaining nooks and crannies of the hydrometeor, resulting in a dense body of ice. Hailstones can grow to large sizes (10 cm diameter or greater) in severe storms.

When the freezing level is far enough above the surface, most precipitation particles melt and thus form raindrops before they reach the surface. The exception is large hailstones. These hydrometeors can fall without melting

through a thick layer of above-freezing air, due to their large size and resulting thermal inertia.

Time scale for particle collisions

Let us attempt to calculate the time between collisions of cloud droplets. In order to collide at all, droplets must have different radii, so as to have different fall speeds. Assuming at first that air flow perturbations around drops cause no deviations in drop trajectories, a cloud droplet of radius a will collide with a droplet of radius b if the latter droplet is located within a horizontal distance $a+b$ of a vertical line passing through the center of the first droplet. The differential speed between the two droplets will be $|w_T(a)-w_T(b)|$, which means that the effective volume swept out per unit time by the first drop in encounters with droplets of radius b is $\pi(a+b)^2|w_T(a)-w_T(b)|$. If there are $N(b)db$ particles with radius between b and $b+db$, then the rate at which the initial particle encounters these particles is $\pi(a+b)^2|w_T(a)-w_T(b)|N(b)db$.

In actuality, aerodynamic forces tend to sweep each particle around the other, thus avoiding a collision. This reduction in the collision rate over the geometrically specified value is accounted for by multiplying the above collision rate by a correction $E(a,b)$ called the *collision efficiency*. The collision efficiency is a strong function of the radii of the two droplets. Since what we are generally interested in is not just the collision rate, but the rate at which the droplets coalesce, we can include the efficiency for coalescence in E as well, at which point we call E the *collection efficiency*. Integrating over all radii for the second particle, we come up with an overall collection rate, which we express as the inverse of a time constant τ:

$$\tau^{-1} = \int_0^\infty \pi(a+b)^2 E(a,b)|w_T(a)-w_T(b)|N(b)db. \tag{5.38}$$

This time constant is a good indication of the ability of a convective cloud to initiate warm rain. If the time constant is comparable to the lifetime of a cloud, then precipitation can occur. The first set of collisions is the hardest, as increased particle sizes result in larger terminal velocities and collection efficiencies. On the other hand, if this time constant is much larger than a cloud lifetime, then precipitation is unlikely to form in significant quantities.

Collection efficiencies are complicated to calculate theoretically and to determine experimentally. In addition to terminal velocity differences, turbulence can bring particles into close enough proximity to coalesce. However,

as a general rule, for both particles having radii greater than 50 μm, collection efficiencies are of order unity. For particles of radius ≈ 20 μm, collection efficiencies are of order 0.1, while for smaller particles than this, collection efficiencies decrease strongly with decreasing radius. Thus, for warm rain to occur, it is important for droplets to grow to as large a size as possible by diffusion (see Pruppacher and Klett, 1978).

Time scales for collisions of non-spherical particles such as ice crystals are even more complex to determine than for spherical droplets.

5.4 Evaporation and breakup of raindrops

Evaporation is like diffusional growth in reverse, except the large drop size means that a ventilation factor must be included. This ventilation factor takes the form of a multiplicative term in the droplet growth equation:

$$a\frac{da}{dt} = \frac{r_S D(\rho/\rho_w)(\mathcal{H} - \mathcal{H}_e)(1 + F\mathrm{Re}^{1/2})}{1 + r_S(D/\kappa)[L_L^2/(C_{PD}R_V T^2)]}, \tag{5.39}$$

where the Reynolds number Re is defined as previously, and where $F = F(\mathrm{Re})$ is a dimensionless quantity which is approximately unity for large Reynolds numbers.

We have already seen that drops larger than a certain size are likely to break up. Repeated growth-breakup cycles tend to result in an exponential drop size distribution first discovered by Marshall and Palmer (1948). This takes the form

$$N(a) = N_0 \exp(-\lambda a), \tag{5.40}$$

where $N(a)da$ is the number of raindrops per unit volume with radius between a and $a + da$. Empirically, $N_0 \approx 1.6 \times 10^7$ m^{-4} and λ is adjusted to produce the observed mass of rain water per unit volume of air. It should be emphasized that this is an empirical result averaged over many rain events and is not necessarily replicated in every case.

5.5 References

Beard, K. V., 1976: Terminal velocity and shape of cloud and precipitation drops aloft. *J. Atmos. Sci.*, **33**, 851-864.

Gunn, R. and G. D. Kinzer, 1949: The terminal velocity of fall for water drops in stagnant air. *J. Meteor.*, **6**, 243-248. The original source on raindrop fall speed.

Hallett, J., and S. C. Mossop, 1974: Production of secondary ice particles during the riming process. *Nature,* **249**, 26-28.

Marshall, J. S., and W. M. Palmer, 1948: The distribution of raindrops with size. *J. Meteor.*, **5**, 165-166.

Pruppacher, H. R., and J. D. Klett, 1978: *Microphysics of clouds and precipitation.* D. Reidel, Dordrecht, 714 pp. This monograph provides encyclopedic coverage of cloud microphysics, and is an excellent reference.

5.6 Problems

1. Derive equations for the activation radius and saturation humidity of soluble aerosols as a function of a_k and a_s. Plot these as a function of a_s over the range 10^{-8} m to 10^{-6} m with a_k calculated for a temperature of 273 K.

2. Suppose the soluble aerosol consists of N particles per unit volume of air, all with the same value of a_s, and hence $\mathcal{H}_e$, in a parcel ascending such that dr_S/dt remains constant (and negative). This supplies condensate to the aerosols at the approximate rate $-dr_S/dt$, assuming that the relative humidity in the parcel never greatly exceeds unity.

   (a) Determine the radius $a(t)$ of the resulting droplets as a function of time.

   (b) Find $\mathcal{H} - \mathcal{H}_e$ as a function of time. You may assume that ρ, T, and r_S remain effectively constant for the purpose of evaluating the right side of equation (5.22).

   (c) For 200 aerosol particles per cubic centimeter, pressure 900 hPa, temperature 290 K, and $dr_S/dt = -10^{-5}$ s^{-1} (equivalent to an updraft of roughly 5 m s^{-1}), plot $a(t)$ and $\mathcal{H} - \mathcal{H}_e$ as a function of time for the first 100 s. (Ignore the changes in all quantities except $\mathcal{H} - \mathcal{H}_e$ in this 500 m ascent.)

(d) Do the same as above for 10000 aerosol particles per cubic centimeter.

3. Suppose a cloud contains two groups of drops, the first with initial radius 5×10^{-6} m, the second with initial radius 1×10^{-6} m. Both groups of drops are supplied with the same constant value of $\mathcal{H} - \mathcal{H}_e$. What will the radius of the second group of drops be when the first group has reached 10×10^{-6} m?

4. Estimate the diffusional growth rate of a spherical ice crystal (a rather rare critter!) of radius a at temperature $T = -5$ C and pressure $p =$ 500 hPa, assuming a vapor pressure equal to water saturation at that temperature. Compute how long such a crystal takes to grow from zero to 50×10^{-6} m radius.

5. Estimate the terminal fall speed of hailstones 6 cm in diameter. Assume that they are solid ice spheres.

6. Obtain an expression for τ (the time constant for droplet collisions) for a droplet of radius a, otherwise assuming a delta function distribution of droplets $N(b) = N_0\delta(b - b_0)$. Take $a = 2b_0$ and assume a constant collection efficiency of $E = 0.1$. Assume the low Re regime for computing terminal velocity.

   (a) Compute the value of τ for a liquid water mass per unit volume of air $\rho_L = 3$ g m^{-3} spread uniformly over 200 condensation nuclei per cubic centimeter.

   (b) Do the same for 3 g m^{-3} of liquid water spread over 5000 nuclei per cubic centimeter.